Analyst

Cite this: *Analyst*, 2012, **137**, 5346

www.rsc.org/analyst

PAPER

Selective determination of cysteine using BSA-stabilized gold nanoclusters with red emission

Ma-Lin Cui,[a] Jia-Ming Liu,*[a] Xin-Xing Wang,[a] Li-Ping Lin,[a] Li Jiao,[a] Li-Hong Zhang,[b] Zhi-Yong Zheng[b] and Shao-Qin Lin[c]

Received 12th July 2012, Accepted 13th September 2012
DOI: 10.1039/c2an36284h

Gold nanoclusters (AuNCs) were synthesized by a macromolecules template using bovine serum albumin (BSA) as stabilizer which can emit red photoluminescence under illumination of ultraviolet light. The fluorescence intensity of AuNCs enhanced through decreasing the surface defects of AuNCs modified with cysteine, herein we present a novel fluorometry for determination of trace cysteine. This method with a wider linear range from 2.0 to 800 nmol mL^{-1}, higher sensitivity (detection limit was 1.2 nmol mL^{-1}) and better selectivity has been utilized to determine cysteine content in real samples, and the results were in a good agreement with those determined by electrochemical biosensor. At the same time, the structures of AuNCs and AuNCs–cysteine were characterized by Fourier-transform infrared spectroscopy (FTIR) and high resolution transmission electron microscopy (HRTEM) and the mechanism of the proposed assay for the detection of cysteine has been discussed.

1. Introduction

As a sulfur-containing amino acid, cysteine plays a crucial biological role in the human body, such as the synthesis of DNA, protein folding, detoxification of cytotoxicity, cell–cell signal transmission and so on.[1] Certain diseases could also be diagnosed resorting to the concentration of cysteine in serum (the concentration of cysteine in healthy serum ranged from 152.8 to 266.5 nmol mL^{-1}).[2] Deficiency of cysteine would lead to a hematopoiesis decrease, leucocyte loss and psoriasis generation,[3] while excessive cysteine will incur in Alzheimer's disease, Parkinson's disease and autoimmune deficiency syndrome.[2,4] In the pervious literature, colorimetric method,[1,5] fluorescence spectrophotometry,[3,6,7] electrochemistry[8–12] and high performance liquid chromatography[13,14] have been proposed for the determination of trace cysteine in different samples. Many of these analytical methods can achieve good sensitivity. However, they require complicated instrumentation and cumbersome laboratory procedures. Moreover, the use of Hg^{2+} (ref. 1) and aldehyde[7] can cause serious environmental pollution, which limits the scope of their practical applications. Therefore, it should be highly desirable to develop a promising method for simple, low-cost, and rapid tracking of cysteine to overcome most of such difficulties. Recently, AuNCs consisting of 25 gold atoms were synthesized *via* a one-step synthesis, which possessed molecular-like properties such as luminescence and unique charging properties due to the size regime is comparable to the Fermi wavelength of the conduction electrons.[15] Furthermore, the applications of AuNCs in the detection of Cu^{2+},[16,17] Hg^{2+},[18,19] CH_3Hg^+,[20] trypsin,[21] melamine[22] and phosphate-containing metabolites[23] have achieved new progress. In particular, our strategies to detect cysteine *via* fluorescent AuNCs have rarely been reported to the best of our knowledge. Obviously, exploring a sensitive, selective, accurate, simple and rapid method for the detection of cysteine content has a great significance and application value in diagnosis and prediction of clinical diseases.

A new method for the detection of trace cysteine has been proposed on the basis of the enhancement of AuNCs fluorescence signal resulting from the adsorption of AuNCs to cysteine when –SH was bonded to the surface of AuNCs. Compared with the previous methods of ref. 5,7 and 12, this sensitive, accurate, simple, rapid and pollution-free fluorometry not only could be used for the detection of trace cysteine in the serum, but also for the diagnosis of human diseases. This research expands the practical applications of AuNCs and promotes the research progress of life sciences.

2. Experimental

2.1 Instrumentation and reagents

A BP-211D electronic analytical balance (Shanghai Mettler-Toledo Instruments Co., Ltd), a DF-101S aggregating heat constant temperature blender with magnetic force (Zhengzhou Great Wall Industry and Trade Co., Ltd), a GL-21M high-speed

[a]*Department of Chemistry and Environmental Science, Zhangzhou Normal College, Zhangzhou, 363000, P. R. China. E-mail: zzsyliujiaming@163.com; Fax: +86 596 2520035; Tel: +86 596 2591352*
[b]*Department of Food and Biological Engineering, Zhangzhou Institute of Technology, Zhangzhou, 363000, P. R. China*
[c]*Department of Biochemistry, Fujian Education College, Fuzhou, 350001, P. R. China*

freezing centrifuge (Saite xiangyi centrifuge Instruments Co., Ltd) and a ZD-A21vacuum freeze drier (Nanjing zaizhi automation Co., Ltd) were used. The acidity of all the systems was measured by the Delta 320 pH meter (Shanghai Mettler-Toledo Instruments Co., Ltd) with a glass electrode. The fluorescence spectra were recorded at a Varian Cary Eclipse fluorescence spectrophotometer with a 1.0 cm quartz cell (Ex slit 20 nm, Em slit 10 nm). High resolution transmission electron microscopy (HRTEM, JEM-2100, Japan electron optics laboratory Co., Ltd) was performed at 200 kV to determine the sizes of AuNCs and AuNCs–cysteine and the structures of AuNCs and AuNCs–cysteine were analyzed by a TENSOR-37 FTIR (Bruker Optics Instruments Co., Ltd).

$HAuCl_4 \cdot 3H_2O$, bovine serum albumin (BSA), NaOH, cysteine, H_3PO_4, CH_3COOH, H_3BO_3, EDTA, perchloric acid (PCA), Tris buffer, 2-mercaptoethanol, 2-chloro-1-methylpyridinium iodide (CMPI) and all other fundamental reagents (analytical-reagent grade) used in this study were purchased from Sinopharm Chemical Reagent Co., Ltd (Shanghai, China). The purities of all chemicals were greater than 99% and were used without further purification. Milli-Q ultrapure water (18.2 MΩ) was used in each experiment.

2.2 Synthesis and characterization of AuNCs

According to the method of ref. 15, 15.00 mL of 10.0 mM $HAuCl_4$ solution was added to 15.00 mL of 50.0 mg mL^{-1} BSA solution under vigorous stirring at 37 °C. Two minutes later, 1.50 mL of 1.0 M NaOH solution was introduced, and the mixture was incubated at 37 °C for 12 h. The color of the solution changed from light yellow to light brown, and then to deep brown. Finally, AuNCs solution was obtained, diluted to 200 mL with ultrapure water and stored at 4 °C for use. AuNCs and AuNCs–cysteine were characterized by FTIR and HRTEM.

2.3 Detection procedure of cysteine

1.00 mL AuNCs and appropriate amount of cysteine were placed in a 10 mL colorimetric tube and 1.00 mL Britton–Robinson buffer (B–R buffer, added 0.2 mol L^{-1} NaOH solution to 100.00 mL mixed solution of 0.04 mol L^{-1} phosphoric acid (H_3PO_4), acetic acid (CH_3COOH) and boric acid (H_3BO_3), and then adjusted to pH 6.00.) of pH 6.00 was added to adjust the acidity of the system. After being diluted to 10.00 mL and quickly mixed, the solution was incubated at 40 °C for 40 min and then cooled down with running water for 5 min. At the same time, the regent blank experiment was carried out. Finally, the fluorescence intensity of the test solution (F_1) and the blank solution (F_0) were recorded, finally, the ΔF ($= F_1 - F_0$) was calculated.

2.4 Sample treatment

According to the reported procedure in ref. 2, 2.00 mL fasting blood was collected by venipuncture from 10 patients to the tube containing 3.6 g EDTA, cooled on ice and centrifuged at 800 r min^{-1} for 20 min. Taken plasma supernatant, 2.00 mL of 1.0 M Tris buffer (pH 8.2), 1.00 mL of 0.10 M EDTA solution and 0.20 mL of 0.10 M 2-mercaptoethanol solution were added. After a 30 min incubation at room temperature, 0.40 mL of 0.10 M CMPI was added, vortex-mixed and kept at room temperature for another 30 min, followed by adding 2.4 mL of 3.0 M PCA solution. The precipitated protein was then removed by centrifugation (at 10 000 r min^{-1} for 10 min), and the supernatant was diluted to 100 mL and stored at 4 °C for use.

3. Results and discussion

3.1 Fluorescence properties of the cysteine detection procedure

As shown in Fig. 1, the fluorescence spectra of AuNCs (curve 3) deviated from BSA (curve 7), and cysteine had slight influence on the fluorescence of BSA (curve 8). AuNCs could emit strong and stable fluorescence at 639.0 nm ($F = 224.4$, curve 3) and B–R buffer (curve 1, $F = 214.8$) showed little influence on AuNCs. However, the fluorescence signal of the system sharply increased in the presence of 8000.0 nmol cysteine and the emission wavelength of the system red shifted for 14.0 nm ($\lambda_{em}^{max} = 644.1$ nm, $F = 317.2$, $\Delta F = 103.9$, curve 5). The phenomena contributed to the fact that cysteine was adsorbed by AuNCs decreasing the surface defects of AuNCs.[24] Additionally, the ΔF of the system was 1.5 times (103.9/69.4) as large as the case in the absence of pH 6.0 B–R buffer indicating that the proper acidity could enhance the fluorescence signal and maintain the stability of the system. Upon the addition of cysteine, the ΔF of the system increased gradually and reached the maximum value when the adsorption capacity of AuNCs reached saturation point. Thus, a fluorometry for cysteine detection has been established based on the linear relationship between the ΔF of the system with cysteine content.

3.2 Optimal conditions for cysteine detection

In order to investigate the sensitivity, precision and selectivity of the analytical method, we explored the effects of the amount of reagent, pH, reaction temperature and time on the ΔF of the system.

3.2.1 Effect of the dosage of AuNCs. Seen from Fig. 2, the ΔF increased with the increasing of the dosage of AuNCs and reached

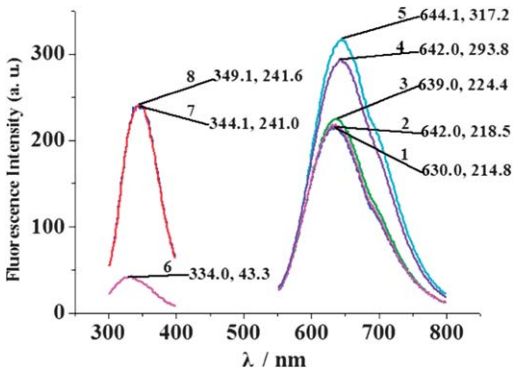

Fig. 1 Fluorescence spectra of AuNCs–cysteine system (1–8 are number of each emission spectra. Two sets of data corresponding 1–8 are emission wavelength and intensity of fluorescence, respectively. The component of each curve presents as follows: 1. 1.00 mL AuNCs + 1.00 mL B–R; 2. 1.00 mL AuNCs + 1.00 mL B–R + 20.0 nmol cysteine; 3. 1.00 mL AuNCs; 4. 1.00 mL AuNCs + 8000.0 nmol cysteine; 5. 1.00 mL AuNCs + 1.00 mL B–R + 8000.0 nmol cysteine; 6. 0.075 mL $HAuCl_4$ + 0.075 mL BSA; 7. 0.075 mL BSA; 8. 0.075 mL BSA + 8000.0 nmol cysteine. The experiments were carried out at 40 °C for 40 min under pH 6.0.).

the maximum when 1.00 mL AuNCs was used, and tended to remain stable with further increase of AuNCs. The reason was that the adsorption capacity of AuNCs reached the maximum and the surface defects of AuNCs came to the minimum.[24] Thus, 1.00 mL AuNCs was chosen for the following study.

3.2.2 Effect of pH value. As shown in Fig. 3, the ΔF of the system increased with pH in the range of pH 5.00–6.00, which was attributed to the decreasing of the surface defects of AuNCs through the adsorption of AuNCs to cysteine when –SH was bonded to the surface of AuNCs. The ΔF reached the maximum at pH 6.00 due to the adsorption capacity becoming the maximum of the AuNCs [25] and kept stable at a pH of 6.00. Thus, B–R buffer solution of pH 6.0 was used in the following work.

3.2.3 Effect of reaction temperature and time. The ΔF of the system increased with the increasing of reaction temperature and reached the maximum at 40 °C, and weakly decreased with the further increase of the temperature (Fig. 4) for 40 min. The reason might be that low temperature was beneficial to the reaction between –SH of cysteine and Au of AuNCs, while the BSA on the surface of AuNCs would denature and aggregate when the reaction temperature exceeded 70 °C. The ΔF reached the maximum for 40 min and then finally approached equilibrium at 40 °C. But the ΔF decreased sharply when the reaction time was more than 50 min (Fig. 5), which was ascribed to partially dissociative adsorption over a long time. Thus, the whole experimental procedure was carried out at 40 °C for 40 min in order to ensure the maximum adsorption on the surface of AuNCs.

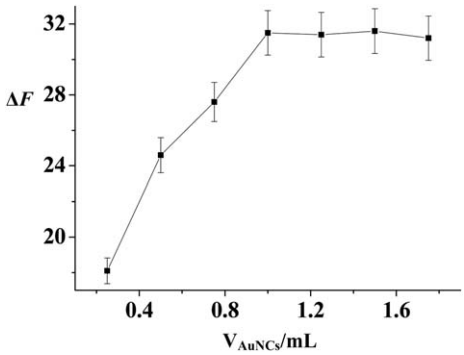

Fig. 2 Effect of the dosage of AuNCs on the ΔF of the AuNCs–cysteine system.

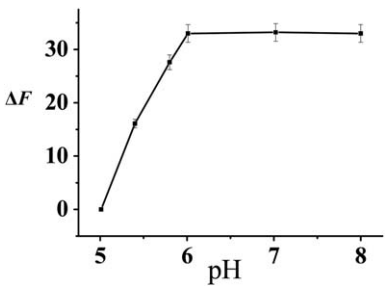

Fig. 3 Effect of pH on the ΔF of the AuNCs–cysteine system.

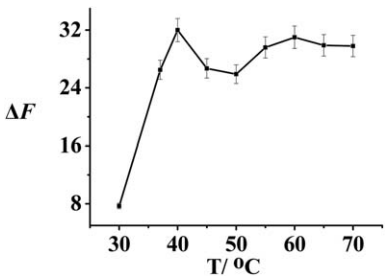

Fig. 4 Effect of reaction temperature on ΔF of the AuNCs–cysteine system.

3.2.4. Stability of the reaction system. When the system stood for 5, 10, 15, 20, 25 and 30 min after being cooled for 5 min with running water, the ΔF values of the system were 33.5, 33.1, 32.9, 33.3, 32.8, and 33.4, respectively. This results shows that the ΔF values of the system were almost constant in 30 min.

3.3 Analytical parameters

As shown in Fig. 6, the corresponding regression equation of the working curve was $\Delta F = 7.120 + 0.1284\ C_{\text{cysteine}}$ nmol mL^{-1}. The linear range, correlation coefficient (r), relative standard deviation (RSD) % (20.0 and 8000.0 nmol cysteine were separately determined in parallel 7 times), detection limit (LD, calculated by 3Sb/k which referred to the quotient between three of the blank

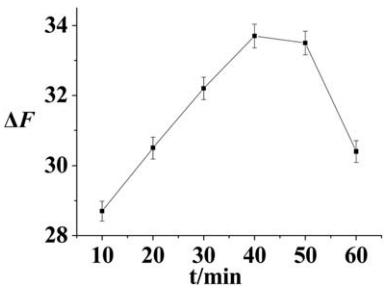

Fig. 5 Effect of reaction time on the ΔF of the AuNCs–cysteine system.

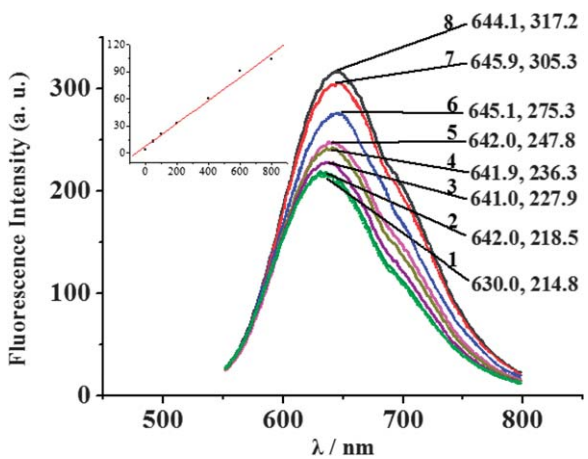

Fig. 6 Representative fluorescence emission spectra of AuNCs in the presence of increasing cysteine concentrations (20.0–8000.0 nmol) in the B–R buffer at pH 6. Inset: fluorescence change (ΔF) titrated with cysteine under the optimum conditions.

Table 1 Linear range, *r*, RSD, LD and LOD

Method	Linear range (nmol mL^{-1})	*r*	RSD (%)	LD (nmol mL^{-1})	LOQ (nmol mL^{-1})
The method	2.0–800.0	0.9948	0.62–0.13	1.2	4.0
Colorimetric assay[5]	4–80			2.5	8.2
Fluorescence method[7]	20–100			1.7	5.6
Electrochemical biosensor method[12]	5–47			4.0	13.2

reagent's standard deviation (Sb = 0.050), the slope of the working curve, $n = 11$) and the limit of quantification (LOQ, calculated by 10Sb/k, $n = 11$) of this method were compared with those of ref. 5, 7 and 12, respectively. Results are listed in Table 1.

Compared with ref. 5,7 and 12, the new method without acetaldehyde possessed lower LD, higher sensitivity, wider linear range and operated more easily (Table 1). Thus, the method was more suitable for the detection of cysteine in human serum.

3.4 Interference effect

This manuscript researches the detection method of cysteine in human blood serum mainly. The selectivity of the method was evaluated by testing the response of other amino acids to the AuNCs–cysteine system under the optimum conditions in the case of 200 nmol of cysteine. When the relative error exceeded ±5%, the amino acid was considered as an interfering agent (Table 2).

As shown in Table 2, the tolerance ratios (the concentration ratio of coexistence substance to cysteine) of most amino acids exceeded 40 without serious interference. Only cysteine, methionine and glutathione contain –SH in human blood serum. Methionine and glutathione did not interfere with the detection of cysteine, their tolerance ratios exceed 50 fold. Besides, there isn't glutathione in human hair and the ratio of methionine to cysteine is 0.36,[26] indicating that methionine didn't interfere with the detection of cysteine. It is obvious that this method is suitable for the detection of cysteine in human blood serum and hair, possessing high selectivity.

3.5 Sample analysis

In order to test practicability of the method, the detection of cysteine in human serum was carried out according to the experiment procedure after being pre-treated. The standard recovery experiment was also carried out. The results were compared with those obtained from the electrochemical biosensor method[12] and listed in Table 3.

Seen from Table 3 and Table 4, in the case of serum A, B, C, D, E, F, G, H, I and J, the F was 1.74, 1.19, 1.62, 1.87, 1.33, 1.14, 1.15, 1.74, 1.47 and 1.47, respectively, indicating that there was

Table 2 Tolerance ratio of other amino acids for the detection of 200 nmol cysteine under the optimal conditions

Foreign amino acids	Tolerance ratio	Relative error (%)	Foreign amino acids	Tolerance ratio	Relative error (%)
Phenylalanine	100	−1.3	Methionine	50	1.4
Tryptophane	100	2.2	Valine	50	−2.9
Threonine	100	−2.8	Serine	40	−3.8
Isoleucine	100	0.60	Histidine	40	−1.0
Arginine	100	0.97	Glycine	40	2.3
Asparagine	100	−1.3	Glutamine	30	−0.18
Glutathion	100	2.1	Leucine	30	4.5
Alanine	100	−1.8	Aspartic acid	20	−1.6
Tyrosine	50	−0.090	Lysine	10	1.6
Proline	50	4.1	Glutamic acid	10	2.9

Table 3 Content detection of cysteine in the sample solution (the added quantity of cysteine was 10.0 nmol mL^{-1}, $n = 6$)

The method					Electrochemical biosensor[12]	
Sample	Average found (nmol mL^{-1})	Cysteine found (nmol mL^{-1})	Recovery (%)	RSD (%)	Average found (nmol mL^{-1})	Er (%)
A	129.6	9.67	96.7	1.0	130.5	−0.69
B	136.8	10.2	102	0.39	136.8	0
C	146.9	9.80	98.0	0.51	147.3	−0.27
D	156.9	10.2	102	0.31	156.4	0.32
E	175.3	9.94	99.4	0.37	175.5	−0.11
F	196.2	10.2	102	0.46	195.5	0.36
G	234.3	9.90	99.0	0.29	234.1	0.09
H	263.1	10.0	100.0	0.27	263.2	−0.04
I	279.6	9.97	99.7	0.38	279.7	−0.04
J	285.7	10.1	101.0	0.16	285.4	0.11

Table 4 Analysis of the significant differences for determination results ($P = 90\%$, $f = n_1 + n_2 - 2 = 10$, $F_{0.95,10} = 5.05$, $t_{0.90,10} = 1.81$)

	The method ($n = 6$)				Electrochemical biosensor[12] ($n = 6$)			Statistical analysis		
Sample	X_i	$\bar{X}_1$	S_1	RSD (%)	X_i	$\bar{X}_2$	S_2	F	$\bar{S}$	t
A	129.7, 128.9, 130.7, 128.9, 127.9, 131.5	129.6	1.32	1.0	130.5, 131.1, 132.0, 129.8, 130.6, 129.1	130.5	1.00	1.74	1.16	1.34
B	136.5, 137.4, 135.9, 137.2, 136.9, 136.7	136.8	0.54	0.39	136.9, 136.3, 135.9, 137.2, 137.5, 136.7	136.8	0.59	1.19	0.87	0
C	146.8, 145.9, 147.2, 148.0, 146.2, 147.1	146.9	0.75	0.51	147.1, 146.9, 146.5, 147.9, 148.0, 147.1	147.3	0.59	1.62	0.67	1.03
D	157.2, 156.9, 156.1, 157.4, 157.3, 156.7	156.9	0.49	0.31	156.4, 156.2, 156.9, 155.7, 157.3, 155.6	156.4	0.67	1.87	0.58	1.49
E	175.8, 174.9, 175.8, 176.1, 174.5, 174.9	175.3	0.65	0.37	175.1, 174.9, 175.8, 174.5, 176.4, 176.1	175.5	0.75	1.33	0.70	0.49
F	196.7, 195.5, 196.9, 194.8, 196.3, 197.1	196.2	0.90	0.46	195.7, 195.6, 194.8, 196.2, 196.5, 193.9	195.5	0.96	1.14	0.93	1.30
G	234.9, 234.8, 235.2, 235.5, 234.8, 234.6	234.3	0.67	0.29	234.1, 234.6, 233.8, 235.0, 232.9, 234.0	234.1	0.72	1.15	0.70	0.49
H	263.3, 262.9, 262.8, 264.3, 263.1, 262.2	263.1	0.70	0.27	263.2, 263.5, 263.1, 262.8, 264.1, 262.6	263.2	0.53	1.74	0.62	0.28
I	279.8, 279.6, 278.5, 280.5, 281.0, 278.3	279.6	1.07	0.38	278.9, 279.6, 279.8, 278.8, 280.3, 280.6	279.7	0.73	1.47	0.9	0.19
J	285.7, 285.4, 285.9, 286.0, 284.9, 286.2	285.7	0.47	0.16	285.3, 286.1, 284.9, 286.0, 284.7, 285.6	285.4	0.57	1.47	0.52	1.00

no significant differences between S_1 and S_2, and t was 1.34, 0, 1.03, 1.49, 0.49, 1.30, 0.49, 0.28, 0.19 and 1.00, respectively, indicating that there was also no significant differences between $\bar{X}_1$ and $\bar{X}_2$. Besides, compared with the electrochemical biosensor method, the relative error was less than ±5% and the recovery was 99.4–101.1% revealing the higher accuracy. The amount of cysteine in D–H human blood serum was within 152.8–266.5 nmol mL^{-1} indicating that patients had recovered their health, while that in A–C human blood serum were less than 152.8 nmol mL^{-1} and in I and J human blood serum was more than 266.5 nmol mL^{-1} indicating that patients were unhealthy and needed the further treatment.

3.6 Mechanisms of synthesis of AuNCs and the detection of cysteine

Upon adding Au(III) ions to the aqueous BSA solution, the protein molecules sequestered Au(III) ions and entrapped them,[27,28] and then the product formed (Scheme 1). The new products were proved to be AuNCs from the HRTEM (Fig. 7a) of products. Cysteine was adsorbed on the surface of AuNCs through the bonding between –SH in cysteine molecule and Au of AuNCs to form AuNCs–cysteine (Scheme 1). Seen from Fig. 7b, the change of sizes implied the formation of AuNCs–cysteine compound also. Consequently, the surface defects of AuNCs decreased[24] and the fluorescence signal of the system enhanced. Based on the linear relationship between the ΔF of the system and the cysteine content, trace cysteine could be detected by florescence enhancement method. Scheme 1 displays the mechanisms of synthesis of AuNCs and the detection of cysteine.

3.7 Morphological characterization of AuNCs and AuNCs–cysteine

Representative HRTEM images of AuNCs (Fig. 7a) and AuNCs–cysteine (Fig. 7b) revealed the presence of clearly

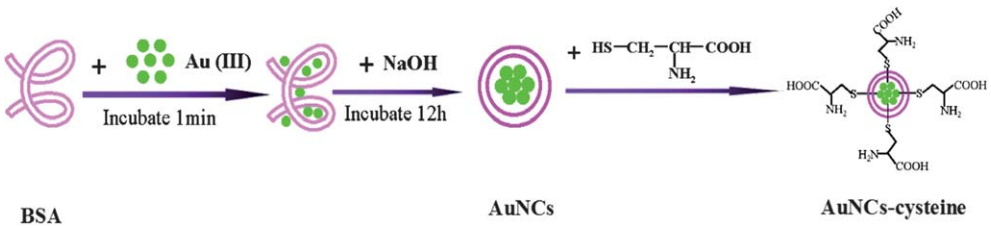

Scheme 1 Mechanisms of synthesis of AuNCs and detection of cysteine.

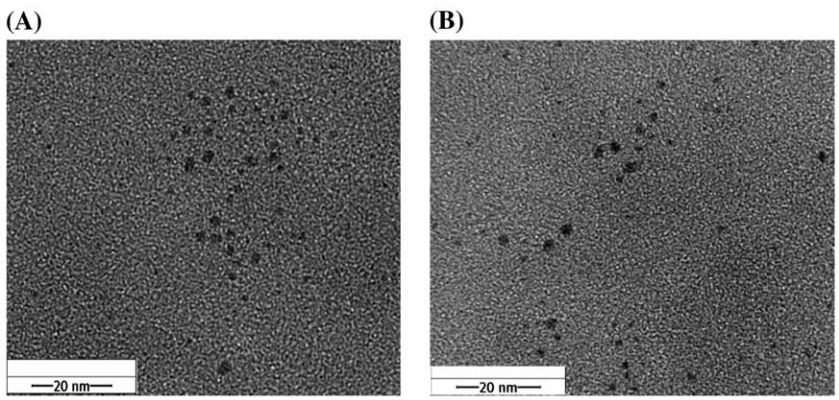

Fig. 7 (a) HRTEM image of AuNCs (b) HRTEM image of AuNCs–cysteine.

Table 5 Infrared spectra data (cm^{-1})

Compounds	$-NH_2$	–OH	–SH	C=O	–NH	$-CH_2$	–CH–	$-CH_3$
AuNCs	ν: 3421.36	ν: 3421.36		ν: 1650.49	δ: 1537.89 ρ: 617.48	ρ: 2963.11		ρ: 1401.94
Cysteine	ν: 3416.28	ν: 3425.57	ν: 2550.47	ν: 1720.62		δ: 1302.34 δ: 1298.16 δ: 1268.73	δ: 1340.52	
AuNCs–cysteine	ν: 3420.82	ν: 3428.45		ν: 1730.56	δ: 1545.23 ρ: 619.35	ρ: 2967.41 δ: 1307.23 δ: 1301.16 δ: 1272.52	δ: 1342.19	ρ: 1406.32

defined features of an average size of ~2 nm and 3 nm, respectively, indicating the successful synthesis of AuNCs and the reaction between AuNCs and cysteine.

In order to prove the probability of reaction occurring between cysteine and AuNCs, the infrared spectra of AuNCs, cysteine and AuNCs–cysteine were scanned by TENSOR-37 infrared spectrometer (KBr pellet) ranging from 200 cm^{-1} to 4000 cm^{-1}.

Table 5 shows the characteristic absorption peaks of the synthesized products that are consistent with that of in ref. 15–25, 27, 29–31, indicating that the products were AuNCs. Therefore, the characteristic absorption peak of ν_{-SH} in AuNCs–cysteine disappeared and the characteristic absorption peaks of $\nu_{C=O}$ and ν_{NH2} red shifted while the characteristic absorption peak of other groups had little change, which proved the possibility of the occurrence for the reaction between the S of –SH in cysteine and the Au in AuNCs.

4. Conclusion

AuNCs were synthesized and their structures were characterized by FTIR and HRTEM in this work. A sensitive, accurate, simple and rapid detection strategy for cysteine has been developed based on the fact that cysteine could decrease the surface defects of AuNCs and enhance the fluorescence signal. This study not only provided a new technology for the detection of trace cysteine in human blood serum and the disease diagnosis, but also promoted the mutual permeation and development between AuNCs and fluorescence spectrometry.

Acknowledgements

This work was supported by Fujian Province Natural Science Foundation (Grant no. 2010J01053 and JK2010035), Fujian Province Education Committee (JA11164, JA11311, JA10203, JA10277 and FJQI 2011006) and the Scientific Research Program of Zhangzhou Institute of Technology Foundation (Grant no. ZZY 1106 and ZZY 1014).

References

1 J. S. Lee, P. A. Ulmann, M. S. Han and C. A. Mirkin, *Nano Lett.*, 2008, **8**, 529–533.
2 G. Chwatko and E. Bald, *Talanta*, 2000, **52**, 509–515.
3 M. Zhang, M. X. Yu, F. Y. Li, M. M. Zhu, M. Y. Li, Y. H. Gao, L. Li, Z. Q. Liu, J. P. Zhang, D. Q. Zhang, T. Yi and C. H. Huang, *J. Am. Chem. Soc.*, 2007, **129**, 10322–10323.
4 W. Y. Lin, L. L. Long, L. Yuan, Z. M. Cao, B. B. Chen and W. Tan, *Org. Lett.*, 2008, **10**, 5577–5580.
5 O. Rusin, N. N. S. Luce, R. A. Agbaria, J. O. Escobedo, S. Jiang, I. M. Warner, F. B. Dawan, K. Lian and R. M. Strongin, *J. Am. Chem. Soc.*, 2004, **126**, 438–439.
6 W. Wang, O. Rusin, X. Xu, K. K. Kim, J. O. Escobedo, S. O. Fakayode, K. A. Fletcher, M. Lowry, C. M. Schowalter, C. M. Lawrence, F. R. Fronczek, I. M. Warner and R. M. Strongin, *J. Am. Chem. Soc.*, 2005, **127**, 15949–15958.
7 F. Tanaka, N. Mase and C. F. Barbas, *Chem. Commun.*, 2004, 1762–1763.
8 J. M. Zen, A. S. Kumar and J. C. Chen, *Anal. Chem.*, 2001, **73**, 1169–1175.
9 S. Shahrokhian, *Anal. Chem.*, 2001, **73**, 5972–5978.
10 K. S. Tseng, L. C. Chen and K. C. Ho, *Electroanalysis*, 2006, **18**, 1306–1312.
11 Y. D. Zhao, W. D. Zhang, H. Chen and Q. M Luo, *Sens. Actuators, B*, 2003, **92**, 279–285.
12 G. Hignett, S. Threlfell, A. J. Wain, N. S. Lawrence, S. J. Wilkins, J. Davis, R. G. Compton and M. F. Cardosi, *Analyst*, 2001, **126**, 353–357.
13 Y. V. Tcherkas and A. D. Denisenko, *J. Chromatogr., A*, 2001, **913**, 309–313.
14 C. M. Pfeiffer, D. L. Huff and E. W. Gunter, *Clin. Chem.*, 1999, **45**, 290–292.
15 J. P. Xie, Y. G. Zheng and J. Y. Ying, *J. Am. Chem. Soc.*, 2009, **131**, 888–889.
16 H. Y. Liu, X. Zhang, X. M. Wu, L. P. Jiang, C. Burda and J. J. Zhu, *Chem. Commun.*, 2011, **47**, 4237–4239.
17 C. V. Durgadas, C. P. Sharmaa and K. Sreenivasan, *Analyst*, 2011, **136**, 933–940.
18 D. H. Hu, Z. H. Sheng, P. Gong, P. F. Zhang and L. T. Cai, *Analyst*, 2010, **135**, 1411–1416.
19 H. Kawasaki, K. Yoshimura, K. Hamguchi and R. Arakawa, *Anal. Sci.*, 2011, **27**, 591–596.
20 Y. H. Lin and W. L. Tseng, *Anal. Chem.*, 2010, **82**, 9194–9200.
21 L. Z. Hu, S. Han, S. Parveen, Y. L. Yuan, L. Zhang and G. B. Xu, *Biosens. Bioelectron.*, 2012, **32**, 297–299.
22 S. Han, S. Y. Zhu, Z. Y. Liu, L. Z. Hu, S. Parveen and G. B. Xu, *Biosens. Bioelectron.*, 2012, **36**, 267–270.
23 P. H. Li, J. Y. Lin, C. T. Chen, W. R. Ciou, P. H. Chan, L. Y. Luo, H. Y. Hsu, E. W. G. Diau and Y. C. Chen, *Anal. Chem.*, 2012, **84**, 5484–5488.
24 L. L. Xóchitl, L. A. Pérez and I. L. Garzón, *Phys. Rev. Lett.*, 2006, **97**, 3401.
25 H. Niu and B. Volesky, *J. Chem. Technol. Biotechnol.*, 2000, **75**, 436–442.
26 C. R. Robbins and C. H. Kelly, *Text. Res. J.*, 1970, **40**, 891–896.
27 L. Yan, Y. Q. Cai, B. Z. Zheng, H. Y. Yuan, Y. Guo, D. Xiao and M. M. F. Choi, *J. Mater. Chem.*, 2012, **22**, 1000–1005.
28 L. Shang, S. J. Dong and G. U. Nienhausa, *Nano Today*, 2011, **6**, 401–418.
29 X. L. Guével, B. Hotzer, G. Jung and M. Schneider, *J. Mater. Chem.*, 2011, **21**, 2974–2981.
30 Y. Chen, Y. Y. Shen, D. Sun, H. Y. Zhang, D. B. Tian, J. R. Zhang and J. J. Zhu, *Chem. Commun.*, 2011, **47**, 11733–11735.
31 A. Retnakumari, S. Setua, D. Menon, P. Ravindran, H. Muhammed, T. Pradeep, S. Nair and M. Koyakutty, *Nanotechnology*, 2010, **21**, 1–12.